

## Magnetic Resonance Imaging (MRI) under pressure – MRI in basic barometrical research

Kasper Hansen<sup>1,2</sup>, Esben Szocska Hansen<sup>1</sup>, Martin Colliander Kristensen<sup>3</sup>, and Michael Pedersen<sup>1,4</sup>

<sup>1</sup>MR Research Centre, Aarhus University Hospital, Aarhus N, DK, Denmark, <sup>2</sup>Dept. of Clinical Medicine, Aarhus University Hospital, Aarhus N, DK, Denmark,

<sup>3</sup>Dept. of Procurement & Clinical Engineering, Region Midt, Aarhus N, Denmark, <sup>4</sup>Dept. of Clinical Medicine, Aarhus University Hospital, Aarhus N, Denmark

**Introduction:** Molecular oxygen has two unpaired electrons and is therefore paramagnetic, whereas most other gasses are not. This phenomenon explains why relaxation times ( $T_1$ ,  $T_2$ ) of tissue and blood have shown to correlate with changes in the inspiratory oxygen level (up to 100%). In a pressure chamber, however, the partial pressure of any gas can be increased markedly, allowing a significant increase in the gas content in the body according to its equilibrium with the partial pressure inside the chamber. Note that though gaseous oxygen is paramagnetic, these molecules are moving too fast to be affected by the MRI magnet. In contrary, its' intermediate dipol-dipol interactions with protons should add a linearly dependent contribution to the relaxation rate in accordance with Solomon-Bloembergen equations, and if this hypothesis is valid, we would expect a pressure-specific  $T_1$ -relaxivity when oxygen is added, but not with other (diamagnetic) gasses. The aim of this study was to evaluate the pressure-specific  $T_1$ -relaxivity of liquids subjected to various gas tensions (oxygen, helium and nitrogen), using a home-built MRI-compatible pressure chamber.

**Methods:** A pressure chamber (range 1 – 12 ATA) was constructed from nonmagnetic materials (Figure 1). The effect of hyperbaric conditions on  $T_1$  values was investigated using phantoms: vials of  $MnCl_2$  (0-3.2 mM) in 10 mM HCl, gadolinium-enriched degassed water or olive oil. MRI was performed with a 3 T Siemens system, and  $T_1$  measurements were performed with a Look-Locker approach at 1, 2, 4, 6, 8, 10, 12 ATA pressurization with atmospheric air, oxygen, nitrogen and helium.  $T_1$  values were derived on a pixel-by-pixel level using a standard NNLS (non-negative least squares) fitting algorithm. For comparison,  $T_2$  values were measured as well, using a multi-echo spin-echo sequence with subsequent exponential fitting.  $T_1$  and  $T_2$  relaxivities were calculated from the  $1/T_1$  (or  $1/T_2$ ) vs. Gd-concentration relationship.

**Results and Discussions:** In this study, we validated an MRI-compatible pressure chamber. The system allows for uncompromised imaging during pressurization. During pressurization with atmospheric air, measurements of  $T_1$  in the  $MnCl_2$  vials provided a  $T_1$ -relaxivity of  $0.31 \text{ s}^{-1} \text{ATA}^{-1}$ , (Figure 2) and a  $T_2$ -relaxivity of  $-0.18 \text{ s}^{-1} \text{ATA}^{-1}$ .

The observed non-zero pressure-specific  $T_1$ - and  $T_2$ -relaxivity constants indicate that the partial pressure of oxygen itself contributes to the magnetic relaxation of protons, and consequently are to be accounted for in future MRI study subjected to hyperbaric conditions. The underlying physiology during and following hypo/hyperbaric conditions is poorly understood, largely as a consequence of inaccessibility of a model animal inside a pressure chamber. Our results form the basis for a novel imaging based research approach in barometric research, aiming to use medical imaging methods to study physiological effect of barometrical exposure of animal-models. We predict that our system will become valuable for basic research in anesthesiology, radiation therapy, hyperbaric oxygen therapy, height-, aviation- and space physiology as well as diving physiology.

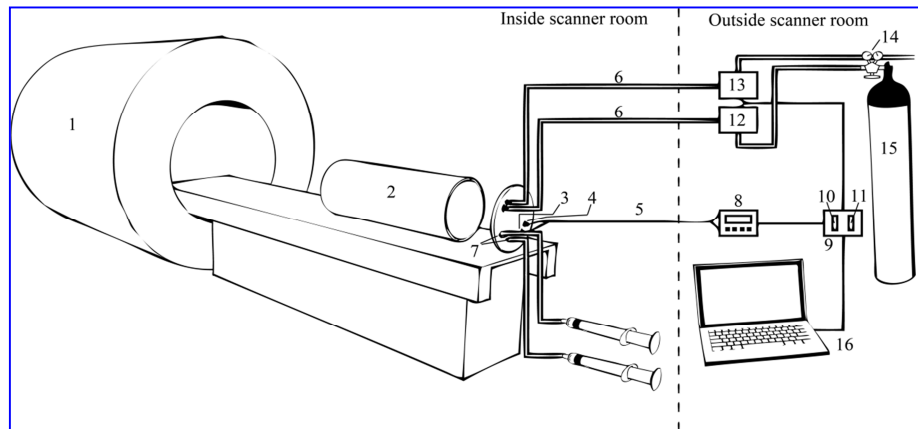


**Figure 1.** MRI, 2. Imaging compatible pressure chamber for small animals (L: 400 mm, Ø: 100 mm, pressure range: 1-12 ATA), 3. Fiber optical pressure sensor (OpSens: OPP-B), 4. Fiber optical temperature sensor (OpSens: OTP-A), 5. Fiber optical cables (7 m), 6. High-pressure gas tubes (20 ATA, 7 m), 7. Pressure tight cable- and catheter lead-ins allowing for arterial and venous access during pressurization, 8. Optical to digital signal converter (OpSens: MultiSens), 9. A/D converter (National Instrument: NI-cDAQ-9188), 10. Sensor output interface (National Instruments: NI-9205), 11. Interface for solenoid valve control (National Instruments: NI-9263), 12. Inlet valve; 2/2-way proportional solenoid valve (Bürkert, proportional solenoid valve; type 2836), 13. Outlet valve; on/off solenoid valve (Bürkert, on/off solenoid valve; type 6013), 14. Pressure reducing valve, 15. Medical gas cylinder (allowing for the use of different gas mixes), 16. Computer system (for pressure profile execution and data acquisition).

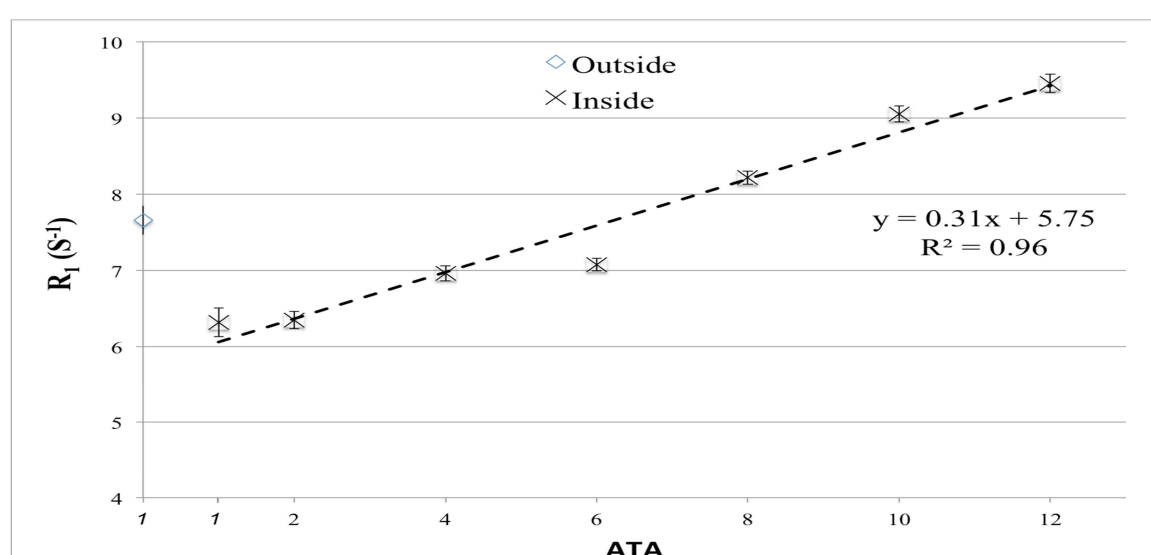


**Figure 2.** Relaxation rate ( $R_1 = 1/T_1$ ) in phantoms consisting of  $MnCl_2$  (0-3.2 mM) in 10 mM HCl as a function of hyperbaric pressure. Atmospheric air was used for pressurization. Pressure-specific  $T_1$ -relaxivity is found from the slope. Note the two 1 ATA values on the x-axis, corresponding to scans at normobaric pressure outside and inside the pressure chamber, respectively.